



THE UNIVERSITY *of* EDINBURGH

Edinburgh Research Explorer

## Ferromagnetism at the interfaces of antiferromagnetic FeRh epilayers

### Citation for published version:

Fan, R, Kinane, CJ, Charlton, TM, De Vries, M, Dorner, P, Ali, M, Brydson, RMD, Marrows, CH, Hickey, BJ, Arena, DA, Tanner, BK, Nisbet, G & Langridge, S 2010, 'Ferromagnetism at the interfaces of antiferromagnetic FeRh epilayers', *Physical review B*, vol. 82, no. 18, 184418, pp. -. <https://doi.org/10.1103/PhysRevB.82.184418>

### Digital Object Identifier (DOI):

[10.1103/PhysRevB.82.184418](https://doi.org/10.1103/PhysRevB.82.184418)

### Link:

[Link to publication record in Edinburgh Research Explorer](#)

### Document Version:

Publisher's PDF, also known as Version of record

### Published In:

Physical review B

### Publisher Rights Statement:

Copyright © 2010 by the American Physical Society. This article may be downloaded for personal use only. Any other use requires prior permission of the author(s) and the American Physical Society.

### General rights

Copyright for the publications made accessible via the Edinburgh Research Explorer is retained by the author(s) and / or other copyright owners and it is a condition of accessing these publications that users recognise and abide by the legal requirements associated with these rights.

### Take down policy

The University of Edinburgh has made every reasonable effort to ensure that Edinburgh Research Explorer content complies with UK legislation. If you believe that the public display of this file breaches copyright please contact [openaccess@ed.ac.uk](mailto:openaccess@ed.ac.uk) providing details, and we will remove access to the work immediately and investigate your claim.



**Ferromagnetism at the interfaces of antiferromagnetic FeRh epilayers**R. Fan,<sup>1,\*</sup> C. J. Kinane,<sup>1</sup> T. R. Charlton,<sup>1</sup> R. Dorner,<sup>2</sup> M. Ali,<sup>2</sup> M. A. de Vries,<sup>2</sup> R. M. D. Brydson,<sup>2</sup> C. H. Marrows,<sup>2</sup> B. J. Hickey,<sup>2</sup> D. A. Arena,<sup>3</sup> B. K. Tanner,<sup>4</sup> G. Nisbet,<sup>5</sup> and S. Langridge<sup>1</sup><sup>1</sup>*ISIS, Harwell Science and Innovation Campus, Science and Technology Facilities Council, Rutherford Appleton Laboratory, Didcot, Oxon OX11 0QX, United Kingdom*<sup>2</sup>*School of Physics and Astronomy, University of Leeds, Leeds, LS2 9JT, United Kingdom*<sup>3</sup>*National Synchrotron Light Source, Brookhaven National Laboratory, Upton, New York 11973-5000, USA*<sup>4</sup>*Department of Physics, Durham University, Durham, DH1 3LE, United Kingdom*<sup>5</sup>*Harwell Science and Innovation Campus, Diamond Light Source Ltd., Didcot, Oxfordshire OX11 0DE, United Kingdom*

(Received 15 July 2010; published 12 November 2010)

The nanoscale magnetic structure of FeRh epilayers has been studied by polarized neutron reflectometry. Epitaxial films with a nominal thickness of 500 Å were grown on MgO (001) substrates via molecular-beam epitaxy and capped with 20 Å of MgO. The FeRh films show a clear transition from the antiferromagnetic (AF) state to the ferromagnetic (FM) state with increasing temperature. Surprisingly the films possess a FM moment even at a temperature 80 K below the AF-FM transition temperature of the film. We have quantified the magnitude and spatial extent of this FM moment, which is confined to within ~60–80 Å of the FeRh near the top and bottom interfaces. These interfacial FM layers account for the unusual effects previously observed in films with thickness <100 Å. Given the delicate energy balance between the AF and FM ground states we suggest a metastable FM state resides near to the interface within an AF matrix. The length scale over which the FM region resides is consistent with the strained regions of the film.

DOI: [10.1103/PhysRevB.82.184418](https://doi.org/10.1103/PhysRevB.82.184418)

PACS number(s): 75.75.-c

**I. INTRODUCTION**

The near-equiatomic  $\alpha'$  phase (CsCl structure) FeRh alloy exhibits a first-order antiferromagnetic (AF) to ferromagnetic (FM) magnetostructural transition just above room temperature (~350 K).<sup>1,2</sup> This transition is accompanied by a volume expansion of ~1% upon entering the FM phase and a temperature hysteresis of ~10 K.<sup>3–5</sup> The FM phase has a collinear structure with 3.2  $\mu_B$  per Fe and 0.9  $\mu_B$  per Rh atom. The antiferromagnetic phase is of *G* type with 3.3  $\mu_B$  per Fe atom and no Rh moment.<sup>6,7</sup> A significant magnetoresistance of 90% was found for bulk FeRh at room temperature and up to 1700% at 4.2 K for polycrystalline FeRh.<sup>8</sup> The transition may be affected and hence controlled by many factors, including the applied magnetic field,<sup>9</sup> ion-irradiation,<sup>10</sup> stress state,<sup>11</sup> and the sample microstructural scale.<sup>12</sup> In nanoscale film form it is of great interest for potential applications in heat-assisted magnetic recording,<sup>13</sup> magnetic refrigeration,<sup>13</sup> and ultrafast (ps) switching.<sup>14</sup> Band-structure calculations by Lounis *et al.*<sup>15</sup> have shown that there is a clear correlation between the thickness of the FeRh thin films and the stability of the FM/AF configuration with ferromagnetism being stabilized for nine atomic layers for a Rh-terminated system. In our previous study, x-ray magnetic circular dichroism (XMCD) showed that FeRh has a finite magnetic moment close to the top surface at room temperature<sup>16</sup> and more recently grazing incident x-ray diffraction shows that a near-surface relaxation occurs at the top interface which could contribute to the stability of the room-temperature FM top surface.<sup>17</sup>

In this work we have employed superconducting quantum interference device (SQUID) magnetometry, x-ray reflectivity/diffraction and polarized neutron reflectivity (PNR) (Refs. 18 and 19) to quantify the magnetization and

structural profile of FeRh epilayers and show that ferromagnetic layers reside at both the top and bottom interfaces.

**II. SAMPLE PREPARATION AND CHARACTERIZATION**

The samples are epilayers grown by molecular-beam epitaxy on MgO single-crystal substrates and are the same as those used in our previous study.<sup>16</sup> The FeRh films have the epitaxial relationship FeRh[100](001)||MgO[110](001). The films are 500 Å thick and were codeposited from separate Fe and Rh sources with a total rate of ~0.3 Å/s. The pressure during growth was  $5 \times 10^{-10}$  Torr and the substrate temperature was 300 °C. The films were postgrowth annealed at 800 °C for 60 min, and then capped *in situ* at 50 °C with 20 Å of MgO.

The thin-film structure was obtained using the Materials and Magnetism beamline I16 at the Diamond Light Source with a photon energy of 10 keV. The low-angle x-ray reflectivity shown in Fig. 1(a) was used to determine the average structure of the thin film. At low angles one is not sensitive to the crystallinity and the electron-density depth profile over the whole sample is analyzed by an optical matrix method.<sup>20</sup> The depth profile is shown as an inset in Fig. 1(a). The substrate interface is sharp with a root-mean-squared roughness of 4.2 Å. The surface/cap region is significantly more diffuse. Given the nature of this interface and the x-ray contrast it is difficult to observe the MgO capping layer. An additional layer with slightly reduced electron density compared to bulk FeRh with thickness of ~60 Å was introduced below the MgO capping layer in order to fully describe the reflectivity data. The FeRh composition was determined by energy-dispersive x-ray spectroscopy on a ~100 nm lamella prepared using focused ion-beam techniques and found to be Fe 44%/Rh 56% with a 3% error.

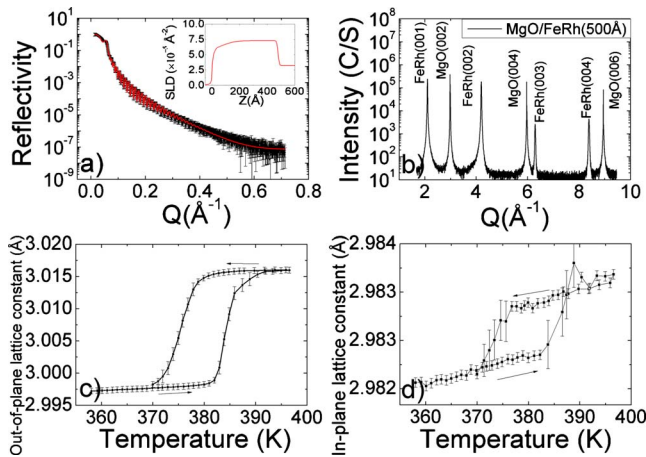


FIG. 1. (Color online) X-ray characterization. (a) The room-temperature low-angle x-ray reflectivity with the best chi-squared fit, (inset) electron density depth profile. (b) The high-angle x-ray diffraction data. (c) Out-of-plane lattice constant as a function of temperature. (d) Temperature-dependence measurement of the bulk in-plane lattice constant across the magnetic transition.

High angle x-ray diffraction data are shown in Fig. 1(b). Clear (001), (002), (003), and (004) reflection peaks of the highly chemically ordered FeRh structure ( $\alpha'$  phase) are observed. The out-of-plane lattice constant at room temperature was calculated from the FeRh (00L) peak positions and has a value of 2.998 Å. This is in good agreement with the bulk value of 2.989 Å reported by Lommel.<sup>2</sup> Furthermore by rotating the sample about an axis perpendicular to the scattering plane, we found the mosaic spread to be  $\sim 0.4^\circ$ . Figure 1(c) shows the out-of-plane lattice constant as a function of temperature, a sharp structural transition is observed consistent with previous bulk<sup>5,21</sup> and thin-film<sup>17</sup> measurements. Figure 1(d) shows the in-plane lattice constant determined from the FeRh (202) reflection as a function of temperature across the magnetic transition. The in-plane lattice constant at room temperature was found to be slightly smaller than the bulk value indicating that the film is compressively strained in-plane by the MgO substrate. The lattice expansion is much smaller compared to that observed in the out-of-plane direction, indicating that the strain from the substrate is restricting the in-plane structural expansion unlike the cubic volume expansion observed in the bulk. Temperature-dependent measurements of the in-plane lattice parameter of the MgO substrate show that it is significantly smaller, 0.1%, than the FeRh in plane. Given that the lattice parameter of the epitaxial FeRh layer is relaxed toward the bulk value, the region close to the MgO interface is substantially compressively strained. At the cap interface the FeRh relaxes extending over a length scale of order 2 nm.<sup>17</sup>

The magnetization was studied using a SQUID magnetometer. Figure 2 indicates that the MgO/FeRh/MgO film has a bulklike transition at around 375 K with a temperature hysteresis of about 10 K consistent with the lattice expansion shown in Fig. 1. The insets are hysteresis loops taken at 300 and 400 K. Comparing the  $M$ - $H$  loops at 400 K and 300 K shows an increase in the coercive field from 30 Oe to 70 Oe, respectively, inline with the typical temperature dependence

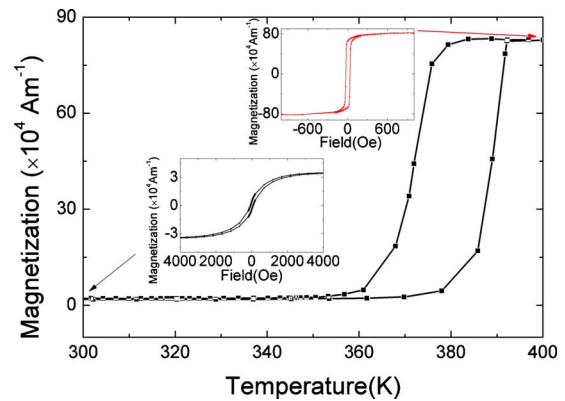


FIG. 2. (Color online) The temperature dependence of the magnetization at an applied field of  $\mu_0 H = 1$  T clearly showing the AF-FM phase transition. The insets show the hysteresis loop measured at 300 and 400 K.

of the anisotropy ( $K_1$ ) of bulk Fe. Qualitatively, the 400 K loop shape is consistent with the sample being ferromagnetic while the 300 K loops can be described by a coexistence of both ferromagnetism and antiferromagnetism.

### III. POLARIZED NEUTRON RESULTS

The magnetic structure of the FeRh film was investigated by PNR using the CRISP reflectometer at ISIS.<sup>22</sup> PNR allows the extraction of the structural and magnetic depth profile in nanoscale systems. The reflectivity is measured as a function of the spin eigenstate of the neutron being either parallel ( $R^\uparrow$ ) or antiparallel ( $R^\downarrow$ ) to a quantization axis defined by the applied magnetic field. From these data the scattering length-density (SLD) profile can be obtained.<sup>19</sup> PNR curves were recorded on the MgO/FeRh/MgO film with an applied field of  $\mu_0 H = 0.34$  T along the MgO (100)/FeRh (110) direction. The experimental results obtained for temperatures above and below the AF-FM transition are shown in Fig. 3. The FeRh film was subdivided into three layers where the struc-

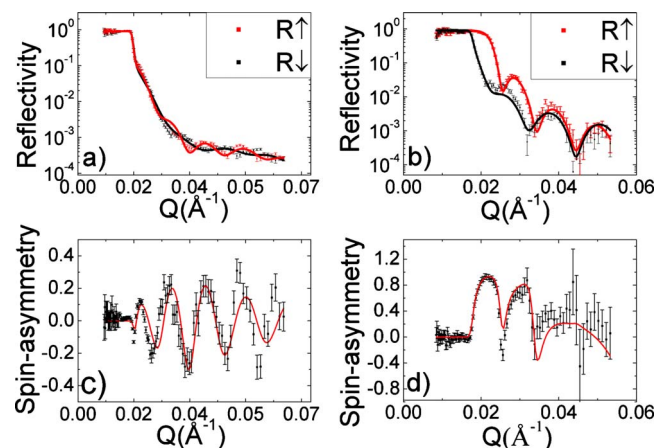


FIG. 3. (Color online) Polarized neutron reflectivity recorded with an applied field of  $\mu_0 H = 0.34$  T at (a) 300 K and (b) 400 K. (c) and (d) are the spin asymmetry at 300 K and 400 K, respectively.

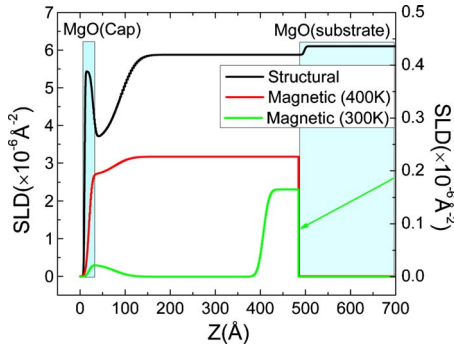


FIG. 4. (Color online) The structural and magnetic profiles for MgO/FeRh/MgO above and below the AF-FM transition temperature. The room-temperature magnetic profile is linked to the right-hand ordinate.

tural and magnetic profiles are allowed to vary independently between the three FeRh layers to account for the possibility of changes in profile at the top and bottom interfaces. However, the structural roughness and structural scattering length density are constrained to be the same for all temperatures. The data at different temperatures were fitted simultaneously<sup>23</sup> using a genetic algorithm and a fine grid slicing model with 101 steps per interface.<sup>24,25</sup> The only free parameters between different temperatures are magnetic in origin. It is worth noting that a uniform single-layer model failed to provide a solution where both sets of reflectivity data (above and below the transition) could be described consistently without a large alteration of the layer thickness or the structural scattering length density, which are both expected to stay approximately the same with temperature, as the volume expansion is on the order of 0.7%. Further justification for a more complex model comes from the spin asymmetry  $(R^\uparrow - R^\downarrow)/(R^\uparrow + R^\downarrow)$  shown in Figs. 3(c) and 3(d). The spin-asymmetry modulation varies markedly above and below the transition temperature indicating that the magnetic layer thickness within the sample changes as the sample is cooled from the FM phase to the AF phase. An AF structure would have a zero spin asymmetry. The extracted structural and magnetic profiles are shown in Fig. 4. The structural profile is consistent with our low-angle x-ray reflectivity analysis allowing for the large elemental difference in scattering lengths for the neutron and x-ray probes. For the magnetic profile there are several interesting features: above the transition temperature the FeRh near the top interface has a magnetic moment of  $1.32 \pm 0.03 \mu_B$  per FeRh slightly smaller than the rest of the FeRh film, which has a magnetic moment of  $1.56 \pm 0.03 \mu_B$  per FeRh. This value is smaller than the bulk value which is  $\approx 2 \mu_B$ . The reduced moment is to be expected as it was shown previously by van Driel *et al.*<sup>11</sup> that thin films have a smaller saturated moment compared to the bulk. Furthermore a slightly Rh-rich composition is also expected to have a smaller saturated moment compared to 50–50 bulk FeRh.<sup>11</sup> At room temperature the spin asymmetry demonstrates clearly that the FeRh has a ferromagnetic component even at a temperature  $\sim 80$  K below the AF-FM transition temperature. More detailed modeling has shown that approximately  $78 \pm 5 \text{ \AA}$  of FeRh close to the MgO substrate remains robustly FM at room tempera-

ture with a magnetic moment of  $\approx 0.08 \pm 0.03 \mu_B$  per FeRh. Similar to the substrate interface, the  $\approx 57 \pm 5 \text{ \AA}$  of FeRh in contact with the MgO capping layer interface remains FM with a magnetic moment of  $0.02 \pm 0.02 \mu_B$ . Clearly this near-surface moment is on the limit of our experimental sensitivity. In modeling the data we also considered ferromagnetic ordering at the cap or substrate interface only. The inclusion of a surface moment only marginally improved the agreement but was included to be consistent with the XMCD data which unambiguously shows a near-surface moment. Within this region it is evident that there is a significant change in composition and interdiffusion between the cap and top  $\approx 100 \text{ \AA}$  of the FeRh film. Away from the interfaces the FeRh thin film has no net magnetic moment at room temperature as expected in the bulk. The observation of a small top-surface FM layer at room temperature is consistent with the finding by Ding *et al.*<sup>16</sup> where a small Fe *K*-edge XMCD signal at room temperature was observed from the same sample. Finally, it is worth comparing our neutron results with the bulk magnetization data obtained using SQUID magnetometry. The average moment per FeRh over the whole sample observed by SQUID at 400 K is  $1.52 \mu_B$  in excellent agreement with our neutron results of  $1.53 \mu_B$  (taking the total moment in all three FeRh layers and averaging over all FeRh atoms within the film). It is known that for our FeRh composition (Fe<sub>44</sub>Rh<sub>56</sub> in the bulk of the film as determined by energy-dispersive x-ray spectroscopy), the saturation magnetization is  $\approx 73\%$  of the 50:50 composition.<sup>11</sup> The extracted magnetization for both the SQUID and neutron measurements is in good quantitative agreement with this reduction. Furthermore, at room temperature our neutron data show that the average moment per FeRh is  $0.02 \mu_B$ , which is again in reasonable agreement with SQUID data where the average moment per FeRh is  $0.04 \mu_B$ .

#### IV. DISCUSSION

We now turn to the origin of the FM regions within the FeRh system. Given the sensitivity of the transition with composition, pressure, magnetic field, etc., several possibilities exist to stabilize the FM regions. The stable room-temperature FM state at the top interface could be accounted for by a mixed phase where different compositions of  $\alpha'$  and/or  $\gamma$  phase FeRh coexist giving rise to a wide range of transition temperatures some of which are below room temperature.<sup>11,26</sup> This deviation from the nominal stoichiometry is consistent with our x-ray and neutron-reflectivity results at the cap/FeRh interface where a change in the structural depth profile near the top 100  $\text{\AA}$  of the interface was observed. This reduction in the structural SLD suggests an Fe-deficient (Rh-rich) layer near the top interface is formed. As mentioned, van Driel *et al.*<sup>11</sup> have shown that Rh-rich FeRh result in a lower saturated moment in the FM phase as well as a reduction in the AF-FM transition temperature. Indeed, Kande *et al.*<sup>27</sup> show room-temperature stable FM for Rh-rich Fe/Rh multilayers. In contrast, no change in the structural depth profile was observed at the substrate interface making this mixed phase an unlikely cause for the FM state at room temperature.



From our x-ray data, at room temperature there is a 0.5% in-plane lattice mismatch between FeRh and the MgO substrate, thereby introducing a compressive strain which, if isotropic, should prevent the onset of the FM state. This is analogous to the observation in high-pressure experiments (and simulation) on bulk FeRh, where pressure-induced compression of the lattice leads to an increase in the AF-FM transition temperature.<sup>28–30</sup> As is demonstrated in this epitaxial system the effective pressure of the substrate and cap is not isotropic and indeed varies in the direction of the surface normal. Although it does not appear to influence the AF-FM transition at 375 K it will result in anisotropic exchange interactions breaking the cubic symmetry observed in the bulk and potentially stabilizing the FM state through a polarization of the Rh atoms. Theoretical studies have highlighted the importance of a Rh moment to the stability of the FM phase. *Ab initio* studies<sup>15,31</sup> for Rh-terminated surfaces indicate a magnetic surface reconstruction favoring a  $p(1 \times 1)$  FM arrangement stable up to nine layers. The termination leads to an increased density of states on the Rh  $d$  electrons leading to a moment on the Rh site. This moment FM coupled to the neighboring Fe helps to reduce the significance of the next-nearest-neighbor AF interactions between the Fe thereby promoting FM ordering. No FM reconstruction is expected for an Fe-terminated surface and the AF structure is the ground state. In this model bulklike moments are calculated for both the Fe and Rh atoms. At finite temperature it is likely that both FM and AF states are populated<sup>32,33</sup> leading to a complex, frustrated interfacial structure. Our measurements indicate a smaller moment at the substrate interface extending over a reasonably long length scale (Fig. 4). Given the codeposition growth it is likely that there exists a distribution of Fe and Rh termination giving rise to regions of FM and AF ordering. This is supported by the shape of the low-temperature SQUID loop (Fig. 2 inset). As PNR averages over the in-plane magnetic induction of the sample the result is a reduced in-plane magnetization as observed. This description is consistent with a nonhomogeneous metamagnetic bulk transition<sup>34,35</sup> for FeRh. The stabilization of the room-temperature FM phase from surface states is appealing but does not satisfactorily account for the long length scale observed for the net polarization. Given that the variation in the in-plane strain along the substrate-film normal extends typically over nanometers it is appealing to connect this to the stability of the FM region. Our results provide an interesting insight into the

long-standing question of why very thin  $<100$  Å FeRh thin film remains FM at room temperature with reduced magnetization.<sup>2,36,37</sup> According to Suzuki *et al.*<sup>36</sup> 10-nm-thick films have a room-temperature magnetization of  $\approx 260 \times 10^3$  A m<sup>-1</sup>. Having extracted the spatial profile from our 50-nm-thick film it is trivial to scale the effective magnetization for a 10 nm film. This scaling, allowing a correction for the compositional moment dependence predicts a magnetization of  $\approx 230 \times 10^3$  A m<sup>-1</sup> consistent with the bulk 10 nm measurements. This supports the view that at room temperature the 80 Å thick AM/FM mixed state is present within the FeRh thin film and as the thickness of the FeRh film is reduced down to and below  $\approx 80$  Å the interfacial AF/FM mixed state becomes the dominate state within the sample and gives rise to the observed ferromagnetism with a reduced net moment.

## V. SUMMARY

To summarize, the magnetic depth profile in a high quality nominally antiferromagnetic epilayer was examined using PNR. Our results show that lattice-constrained FeRh has a small FM moment for both the cap and substrate interfaces at room temperature. Detailed modeling has revealed that this reduced FM moment is mainly confined within 80 Å of FeRh in contact with the interface, suggesting a stable FM layer is present within lattice constrained films. Potentially, this behavior accounts for the observation by several groups of ferromagnetism in nominally antiferromagnetic FeRh. Further investigations to control the anisotropic strain field are underway and we hope the work will stimulate accurate calculations of the effect of anisotropic pressure and realistic interfaces on this intriguing transition. This study highlights the importance of interfacial control and understanding in spintronic systems. Producing heterostructures judiciously combining FeRh with piezoelectric or multiferroic material could offer an alternative route to the nanoscale control of magnetism by an electric field.

## ACKNOWLEDGMENTS

This work was supported by the EPSRC, STFC Center for Materials Physics and Chemistry, the Nuffield Foundation, and Department of Energy Office of Basic Energy Sciences. We would like to thank ISIS and Diamond Light Source Ltd. for the provision of neutron and x-ray beamtime, respectively.

\*raymond.fan@stfc.ac.uk

<sup>1</sup>J. S. Kouvel and C. C. Hartelius, *J. Appl. Phys.* **33**, 1343 (1962).

<sup>2</sup>J. M. Lommel, *J. Appl. Phys.* **37**, 1483 (1966).

<sup>3</sup>L. Zsoldos, *Phys. Status Solidi B* **20**, K25 (1967).

<sup>4</sup>S. Maat, J. U. Thiele, and E. E. Fullerton, *Phys. Rev. B* **72**, 214432 (2005).

<sup>5</sup>M. R. Ibarra and P. A. Algarabel, *Phys. Rev. B* **50**, 4196 (1994).

<sup>6</sup>G. Shirane, C. Chen, and P. Flinn, *Phys. Rev.* **131**, 183 (1963).

<sup>7</sup>G. Shirane, R. Nathans, and C. W. Chen, *Phys. Rev.* **134**, A1547 (1964).

<sup>8</sup>P. A. Algarabel, M. R. Ibarra, C. Marquina, A. del Moral, J. Galibert, M. Iqbal, and S. Askenazy, *Appl. Phys. Lett.* **66**, 3061 (1995), and references therein.

<sup>9</sup>P. Kushwaha, A. Lakhani, R. Rawat, and P. Chaddah, *Phys. Rev. B* **80**, 174413 (2009).

<sup>10</sup>N. Fujita, S. Kosugi, Y. Saitoh, Y. Kaneta, K. Kume, T. Batchu-

- luun, N. Ishikawa, T. Matsui, and A. Iwase, *J. Appl. Phys.* **107**, 09E302 (2010).
- <sup>11</sup>J. van Driel, R. Coehoorn, and G. J. Strijkers, *J. Appl. Phys.* **85**, 1026 (1999).
- <sup>12</sup>K. Kang, A. R. Moodenbaugh, and L. H. Lewis, *Appl. Phys. Lett.* **90**, 153112 (2007).
- <sup>13</sup>J.-U. Thiele, S. Maat, and E. E. Fullerton, *Appl. Phys. Lett.* **82**, 2859 (2003).
- <sup>14</sup>G. Ju, J. Hohlfield, B. Bergman, R. J. M. van de Veerdonk, O. N. Mryasov, J.-Y. Kim, X. Wu, D. Weller, and B. Koopmans, *Phys. Rev. Lett.* **93**, 197403 (2004).
- <sup>15</sup>S. Lounis, M. Benakki, and C. Demangeat, *Phys. Rev. B* **67**, 094432 (2003).
- <sup>16</sup>Y. Ding, D. A. Arena, J. Dvorak, M. Ali, C. J. Kinane, C. H. Marrows, B. J. Hickey, and L. H. Lewis, *J. Appl. Phys.* **103**, 07B515 (2008).
- <sup>17</sup>J. W. Kim, P. Ryan, Y. Ding, L. H. Lewis, C. J. Kinane, B. J. Hickey, C. H. Marrows, M. Ali, and D. A. Arena, *Appl. Phys. Lett.* **95**, 222515 (2009).
- <sup>18</sup>J. F. Ankner and G. P. Felcher, *J. Magn. Magn. Mater.* **200**, 741 (1999).
- <sup>19</sup>S. J. Blundell and J. A. C. Bland, *Phys. Rev. B* **46**, 3391 (1992).
- <sup>20</sup>L. G. Parratt, *Phys. Rev.* **95**, 359 (1954).
- <sup>21</sup>J. M. Lommel and J. S. Kouvel, *J. Appl. Phys.* **38**, 1263 (1967).
- <sup>22</sup><http://www.isis.stfc.ac.uk/instruments/crisp/>.
- <sup>23</sup>P. Kienzle, M. Doucet, D. McGillivray, K. O'Donovan, N. Berk, and C. Majkrzak, 2000–2006, <http://www.ncnr.nist.gov/reflpak>
- <sup>24</sup>C. F. Majkrzak, *Physica B* **221**, 342 (1996).
- <sup>25</sup>C. Majkrzak, K. O'Donovan, and N. Berk, *Neutron Scattering from Magnetic Materials* (Elsevier, New York, 2006).
- <sup>26</sup>S. Inoue, H. Y. Y. Ko, and T. Suzuki, *IEEE Trans. Magn.* **44**, 2875 (2008).
- <sup>27</sup>D. Kande, D. Laughlin, and J.-G. Zhu, *J. Appl. Phys.* **107**, 09E318 (2010).
- <sup>28</sup>A. Hernando, J. M. Barandiarán, J. M. Rojo, and J. C. Gómez-Sal, *J. Magn. Magn. Mater.* **174**, 181 (1997).
- <sup>29</sup>L. Vinokurova, A. Vlasov, N. Kulikov, and M. Pardavi-Horváth, *J. Magn. Magn. Mater.* **25**, 201 (1981).
- <sup>30</sup>M. E. Gruner and P. Entel, *Phase Transitions* **78**, 209 (2005).
- <sup>31</sup>C. Dahmoune, S. Lounis, M. Talanana, M. Benakki, S. Bouarab, and C. Demangeat, *J. Magn. Magn. Mater.* **240**, 368 (2002).
- <sup>32</sup>H. Yamada, H. Shimizu, K. Yamamoto, and K. Uebayashi, *J. Alloys Compd.* **415**, 31 (2006).
- <sup>33</sup>The calculated energy difference between the AF and FM ground states is of order 100 K.
- <sup>34</sup>B. Bergman, G. Ju, J. Hohlfield, R. J. M. van de Veerdonk, J.-Y. Kim, X. Wu, D. Weller, and B. Koopmans, *Phys. Rev. B* **73**, 060407 (2006).
- <sup>35</sup>I. Radu, C. Stamm, N. Pontius, T. Kachel, P. Ramm, J.-U. Thiele, H. A. Dürr, and C. H. Back, *Phys. Rev. B* **81**, 104415 (2010).
- <sup>36</sup>I. Suzuki, T. Koike, M. Itoh, T. Taniyama, and T. Sato, *J. Appl. Phys.* **105**, 07E501 (2009).
- <sup>37</sup>C. Stamm, J.-U. Thiele, T. Kachel, I. Radu, P. Ramm, M. Kosuth, J. Minár, H. Ebert, H. A. Dürr, W. Eberhardt, and C. H. Back, *Phys. Rev. B* **77**, 184401 (2008).